Nonlinear Dynamic Stability of Laminated Beams Subjected to Pulsating Thermal Loads

R. Suresh,* Gajbir Singh,* and G. Venkateswara Rao*
Vikram Sarabhai Space Centre, Trivandrum 625 022, India

Introduction

DURING the past two to three decades, a large amount of literature has been devoted to postbuckling analysis of structures. With such an analysis the actual load-carrying capacity of the structure can be evaluated, and a possible catastrophic failure associated with the secondary equilibrium path can be avoided. Contrary to static buckling of structures, which is fairly well understood, dynamic buckling of autonomous and nonautonomous systems needs requisite attention. The stability of the lateral motion of bars subjected to pulsating periodic axial loads has been reported in Refs. 1–4. The governing differential equation of a simply supported beam is a single equation of the Mathew–Hill type for which the regions of stability and instability indicate the stability and instability of the lateral motion. For cases of arbitrary support conditions, the general approach employed by most of these investigators is one in which either integral equations or the Galerkin method is used to reduce the governing equations of the problem to a single Mathew–Hill equation. The influence of geometric nonlinearity (large amplitudes) on the dynamic stability of bars is investigated by Reiss and Matkowsky[5] and Rubenfield.[6] The nonlinear equations are solved by employing the perturbation method or the method of multiple scales. Brown et al.[7] were among the first few to employ the versatile tool, the finite element method, for computing the regions of instability of bars with various support conditions. However, their study is limited to linear analysis. When employed for geometric nonlinear dynamic buckling analysis, the finite element method not only becomes computationally expensive but also leads to cumbersome equations. The difficulties arise in handling the quadratic and cubic nonlinearities on spatial and temporal variation. In this Note a simple semi-analytical approach is proposed to study the nonlinear dynamic buckling behavior of asymmetrically laminated beams. A two-node laminated beam element with three degrees of freedom per node is developed and employed to obtain the spatial distribution corresponding to the fundamental mode of vibration. The nonlinear finite element equations are reduced to a single nonlinear ordinary differential equation, which in turn is solved by using the Ritz–Galerkin method to compute the regions of instability. The influence of the quadratic nonlinear term is also investigated.

Governing Equations of the Laminated Beam

In this section, von Kármán plate theory, which is a subset of the general nonlinear theory of elasticity, is reduced for laminated beams and employed for the problem formulation. The derivation assumes large displacements, but the rotations and strains are assumed to be small compared to unity. It implies that the change in the geometry in the definition of stresses and integrations is neglected. Further, use is made of Mindlin's assumptions, i.e., planes normal to the undeformed middle surface remain plane though not necessarily normal to the middle surface after deformation. Under these assumptions the kinematics of a plate can be written as

$$\begin{aligned}\bar{u}(x, y, z, \tau) &= u(x, y, \tau) + z\psi_x(x, y, \tau)\\ \bar{v}(x, y, z, \tau) &= v(x, y, \tau) + z\psi_y(x, y, \tau)\\ \bar{w}(x, y, z, \tau) &= w(x, y, \tau)\end{aligned} \tag{1}$$

where $\bar{u}$, $\bar{v}$, and $\bar{w}$ are components of displacement anywhere in the plate in the x, y, and z directions, respectively; u, v, and w denote midplate displacements in the x, y, and z directions, respectively; similarly ψ_x and ψ_y are bending rotations of midplane normal about the y and x axis, respectively; and τ denotes time.

Using Eq. (1), the von Kármán type of nonlinear strain displacement relationship reads as

$$\begin{aligned}\varepsilon_x &= u_{,x} + \tfrac{1}{2}w_{,x}^2 + z\psi_{x,x} - \alpha_x \Delta T\\ \varepsilon_y &= v_{,y} + \tfrac{1}{2}w_{,y}^2 + z\psi_{y,y} - \alpha_y \Delta T\\ \gamma_{xy} &= u_{,y} + v_{,x} + w_{,x}w_{,y} + z(\psi_{x,y} + \psi_{y,x}) - \alpha_{xy}\Delta T\\ \gamma_{xz} &= w_{,x} + \psi_x, \qquad \gamma_{yz} = w_{,y} + \psi_y\end{aligned} \tag{2}$$

where the transverse normal strain ε_z is neglected. The subscript variable following the comma denotes differentiation with respect to that variable; α_x, α_y, and α_{xy} are transformed thermal coefficients of expansion; and ΔT is the temperature difference.

The constitutive relationship for a laminated beam is derived by setting $N_2 = N_6 = M_2 = M_6 = 0$ and substituting ε_2, ε_6, κ_2, and κ_6 in terms of ε_1 and κ_1 in the plate constitutive equation[8–11]; the resulting equation becomes

$$\begin{Bmatrix}\bar{N}_x\\ \bar{M}_x\\ Q_x\end{Bmatrix} = \begin{bmatrix}A^* & B^* & 0\\ B^* & D^* & 0\\ 0 & 0 & S_{44}\end{bmatrix}\begin{Bmatrix}\varepsilon_x\\ \kappa_x\\ \gamma_{xz}\end{Bmatrix} \tag{3}$$

Note that a shear correction factor of value $\frac{5}{6}$ is absorbed in S_{44}, where $\bar{N}_x = N_x + N_x^T$, $\bar{M}_x = M_x + M_x^T$, and N_x^T and M_x^T are thermal stresses and moment resultants, respectively.

The strain energy of the laminated beam can be expressed as

$$U = \frac{b}{2}\int_L (\bar{N}_x\varepsilon_x + \bar{M}_x\kappa_x + \bar{Q}_x\gamma_{xz})\,\mathrm{d}x \tag{4}$$

If the axial ineria of the laminated beam is neglected and all of the layers are assumed to be of same material, then the kinetic energy expression reads as

$$T = \frac{b}{2}\int_L \left(R\dot{w}^2 + I\dot{\psi}_x^2\right) \tag{5}$$

with

$$R = \int_0^h \rho\,\mathrm{d}z, \qquad I = \int_0^h \rho z^2\,\mathrm{d}z$$

where ρ and h are the density of the layer material and the total thickness of the laminate, respectively.

Finite Element Formulation

Let the domain of the laminated beam be divided into a number of two-node beam elements. A linear and cubic variation is assumed for axial and transverse displacements, respectively:

$$u = \alpha_1 + \alpha_2\xi \tag{6}$$

$$w = \beta_1 + \beta_2\xi + \beta_3\xi^2 + \beta_4\xi^3 \tag{7}$$

where α_1, α_2, β_1, β_2, β_3, and β_4 are generalized coordinates and ξ represents a natural coordinate such that $(-1 \le \xi \le 1)$. Making use of the moment shear equilibrium $(M_x' = Q_x)$, we can express the bending rotation ψ_x as

$$\psi_x = -w_{,x} + \left(D_{11}^*/S_{44}\right)\psi_{x,xx} \tag{8}$$

To incorporate Euler beam theory in the case of slender beams, we substitute $\psi_x = -w_{,x}$ in the right-hand side of Eq. (8). Substitution of Eq. (7) in the resulting equation yields

$$\psi_x = \frac{2}{l}\left(-\beta_2 - 2\beta_3\xi - 3\beta_4\xi^2 - 2\eta\beta_4\right), \qquad \eta = \frac{12D_{11}^*}{S_{44}l^2} \tag{9}$$

A close examination of Eqs. (7) and (9) reveals that the variation assumed for ψ_x is one order lower than that of transverse displacement w. This result leads to a consistent shear strain variation. The shear locking in isoparametric finite elements results because of the assumption of the same polynomial variation for w and ψ_x. Thus, it is expected that the variation assumed here leads to a lock-free

Received March 9, 1998; revision received Sept. 26, 1998; accepted for publication Nov. 1, 1998.

*Scientist/Engineer, Structural Engineering Group.

element. Using Eqs. (6), (7), and (9), the field variables u, w, and ψ_x in terms of nodal variables can be written as

$$u = [(1-\xi)/2]u_1 + [(1+\xi)/2]u_2 \tag{10}$$

$$w = N_1 w_1 + N_2 w_2 + N_3 \psi_{x1} + N_4 \psi_{x2} \tag{11}$$

$$\psi_x = M_1 w_1 + M_2 w_2 + M_3 \psi_{x1} + M_4 \psi_{x2} \tag{12}$$

where N_1–N_4 and M_1–M_4 are shape functions. These shape functions can be expressed in terms of natural coordinate ξ and material properties η. Substituting Eqs. (10–12) in the total kinetic potential and following the procedure described by Singh et al.,[9] the following nonlinear dynamic finite element equations are derived:

$$\left[\begin{bmatrix} k_{uu} & k_{uw} \\ k_{wu} & k_{ww} \end{bmatrix} + \begin{bmatrix} 0 & n_{nw1} \\ n_{wu1} & n_{ww1} \end{bmatrix} + \begin{bmatrix} 0 & 0 \\ 0 & n_{ww2} \end{bmatrix} + \lambda \begin{bmatrix} 0 & 0 \\ 0 & k_g \end{bmatrix}\right] \times \begin{Bmatrix} q_u \\ q_w \end{Bmatrix} + \begin{bmatrix} 0 & 0 \\ 0 & m_{ww} \end{bmatrix} \begin{Bmatrix} \ddot{q}_u \\ \ddot{q}_w \end{Bmatrix} = 0 \tag{13}$$

The load parameter λ in Eq. (13) consists of two parts, i.e., $\lambda = \lambda_0 + \lambda_1 \cos\theta t$, where λ_0 is uniform compression and λ_1 is the intensity of the pulsating load.

Solution Procedure

Linear vibration analysis is performed to compute the fundamental frequency and the corresponding mode shape. This mode shape is assumed as the spatial distribution, which is a reasonable approximation for moderately large amplitude, for the nonlinear system of equations (13), i.e.,

$$\{q_w\} = \{\bar{q}_w\} A(t) \tag{14}$$

where $\{\bar{q}_w\}$ is a normalized eigenvector (corresponding to the fundamental frequency) such that maximum transverse displacement because of bending is unity and $A(t)$ represents temporal variation. The axial displacement vector can now be expressed in terms of $\{q_w\}$ by substituting Eq. (14) into Eq. (13) as

$$\{q_u\} = -[k_{uu}]^{-1}[k_{uw}]\{q_w\}A - [k_{uu}]^{-1}[n_{uw1}]\{q_w\}A^2 \tag{15}$$

Making use of Eq. (15), we can rewrite the equation of motion (13) as

$$\begin{aligned} &\left[k_{ww} - k_{wu}k_{uu}^{-1}k_{uw}\right]\{\bar{q}_w\}A + \left[\bar{n}_{ww1} - k_{wu}k_{uu}^{-1}\bar{n}_{uw1}\right. \\ &\left. - \bar{n}_{wu1}k_{uu}^{-1}k_{uw}\right]\{\bar{q}_w\}A^2 + \left[\bar{n}_{ww2} - \bar{n}_{wu1}k_{uu}^{-1}\bar{n}_{uw1}\right]\{\bar{q}_w\}A^3 \\ &+ (\lambda_0 + \lambda_1 \cos\theta t)[k_G]\{\bar{q}_w\}A + [m_{ww}]\{\bar{q}_w\}\ddot{A} = 0 \end{aligned} \tag{16}$$

The bars over the nonlinear stiffness submatrices indicate that the are computed using the normalized eigenmode $\{\bar{q}_w\}$. Premultiplying Eq. (16) with $\{\bar{q}_w\}^T$ and dividing throughout with $[\{\bar{q}_w\}^T[m_{ww}]\{\bar{q}_w\}]$ gives an equation of the form

$$\ddot{A} + \alpha A + \beta A^2 + \gamma A^3 + (r + s\cos\theta t)A = 0 \tag{17}$$

In the absence of β and γ, the nonlinear stiffness coefficients, Eq. (17) reduces to the standard Mathew–Hill equation, the solution of which is well known.[2] Equation (17) is solved using the weighted residual method[12] to obtain the instability boundaries.

Assuming the temporal variations $A = a_1 \cos(\theta t/2)$ and $A = a_1 \sin(\theta t/2)$, we obtain

$$\theta^2/4 = \alpha + (r \pm s/2) + (8/3\pi)\beta a_1 + \tfrac{3}{4}\gamma a_1^2 \tag{18}$$

In the preceding equation + corresponds to the cosine function, whereas − corresponds to the sine function. The dynamic stability region is the area bounded between the surfaces generated by Eq. (18), with the upper and lower bounds corresponding to $(r + 0.5s)$ and $(r - 0.5s)$, respectively.

Numerical Results and Discussion

In this section dynamic instability regions of isotropic, symmetric, and ansymmetric laminated beams with different end conditions are computed and presented in tabular and graphical fashion. A series of example problems is solved to validate the proposed method, and some interesting observations are made.

The mechanical properties considered in this study (high modulus graphite/epoxy laminate tested in the laboratory) are

$$E_L = 335\,\text{GPa}, \qquad E_T = 4\,\text{GPa}$$

$$G_{LT} = G_{LZ} = 3\,\text{GPa}, \qquad \nu_{LT} = 0.28$$

Results in this section are presented in the form of the following nondimensional parameters:

$$A_m = \frac{A_{\max}}{\zeta}, \qquad \zeta = \sqrt{\frac{I}{A}}, \qquad \mu = \frac{s}{2(1-r)}$$

The solutions of Eq. (18) will lead to $\phi_1 = [\theta_1/\omega]$ and $\phi_2 = [\theta_2/\omega]$, which correspond to $(r + 0.5s)$ and $(r - 0.5s)$ of the same equation.

The critical loads and fundamental frequencies of various isotropic and laminated beam configurations were computed and compared with those available in the open literature. The present finite element is found to yield accurate results even with coarse idealization. The details of such comparisons and convergence studies are omitted for the sake of brevity.

Nonlinear Dynamic Stability of Antisymmetric Angle-Ply Beams

In this section nonlinear dynamic stability behavior of short $(L/\zeta = 25)$, asymmetrically laminated [±45 deg] beams with various end conditions is studied in detail. The beams are assumed to be subjected to only pulsating thermal loads $(r = 0, s \neq 0)$. To give better insight, results are presented in the form of tables and three-dimensional plots.

The dynamic stability regions of a composite beam with simply supported (SS) ends is shown in Fig. 1. The numeric data for dynamic stability regions for the SS and fixed (FF) ends are given in Tables 1 and 2. The stability regions of composite beams with both ends SS and both ends FF are the same in the regions of infinitesimal amplitudes $(A_m = 0)$; they are different in the regions of finite amplitudes $(A_m > 0)$. The stability region reduces with the increase in amplitude, and this reduction is more pronounced in the case of SS beams than in the case of FF beams. This reduction in the stability region at $A_m = 2.0$ is 10% and 27% for FF and SS beams, respectively.

Nonlinear Dynamic Stability of Antisymmetric Cross-Ply Beams

In all of the cases studied so far, the nonlinear stiffness coefficient β is zero. To investigate the influence of β on the dynamic stability behavior, a two-layer, cross, ply beam with SS and FF end conditions was examined. A nonzero β exists in the case of SS cross-ply beams; however, it is zero in the case of beams with fixed ends. This happens because the end moments generated due to bending extension coupling are counterbalanced by the reactive end moments in the case of beams with FF ends. Three-dimensional plots (ϕ vs μ vs A_m) for a SS beam are plotted in Fig. 2. The numeric data for SS and FF ends are given in Tables 3 and 4, respectively. This study reveals that a nonlinear free vibration characteristic of ansymmetric beams $(\beta \neq 0)$ is that they oscillate with different amplitudes in positive

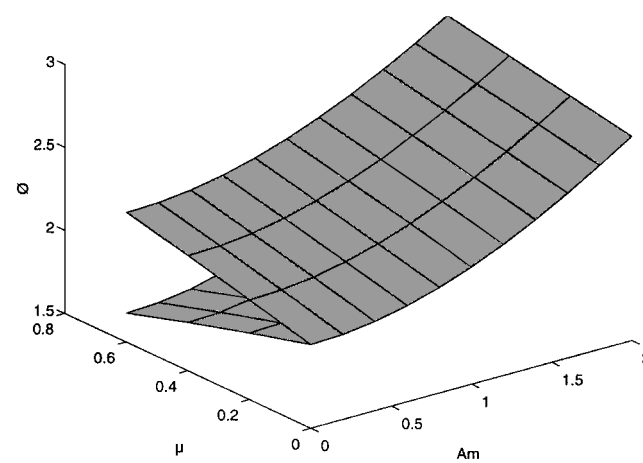

Fig. 1 Variation of ϕ with load parameters μ at various amplitudes for a short ($L/\zeta = 25$) composite beam (asymmetric layup ± 45 deg) with SS ends.

Table 1 Variations of ϕ with load parameter μ at various amplitudes for short (L/ζ = 25) asymmetrical composite beams with simply supported end condition [± 45 deg]

	$\mu = 0.0$		$\mu = 0.2$		$\mu = 0.4$		$\mu = 0.6$	
A_m	ϕ_1	ϕ_2	ϕ_1	ϕ_2	ϕ_1	ϕ_2	ϕ_1	ϕ_2
0	2	2	2.09762	1.89737	2.19089	1.78885	2.28035	1.67332
0.2	2.00862	2.00862	2.10584	1.90645	2.19876	1.79848	2.28791	1.68361
0.4	2.03425	2.03425	2.1303	1.93344	2.2222	1.82707	2.31045	1.71411
0.8	2.13372	2.13372	2.22548	2.03783	2.3136	1.9372	2.39849	1.83105
1.0	2.20537	2.20537	2.29427	2.11274	2.37985	2.01585	2.46245	1.91407
2.0	2.73032	2.73032	2.80262	2.65606	2.87309	2.57966	2.94188	2.50093

Table 2 Variations of ϕ with load parameter μ at various amplitudes for short (L/ζ = 25) asymmetrical composite beams with fixed-end condition [± 45 deg]

	$\mu = 0.0$		$\mu = 0.2$		$\mu = 0.4$		$\mu = 0.6$	
A_m	ϕ_1	ϕ_2	ϕ_1	ϕ_2	ϕ_1	ϕ_2	ϕ_1	ϕ_2
0	2	2	2.09762	1.89737	2.19089	1.78885	2.28035	1.67332
0.2	2.0023	2.0023	2.09981	1.89979	2.19299	1.79142	2.28237	1.67607
0.4	2.00918	2.00918	2.10637	1.90704	2.19927	1.79911	2.2884	1.68428
0.8	2.03646	2.03646	2.13241	1.93576	2.22423	1.82953	2.3124	1.71674
1.0	2.05669	2.05669	2.15174	1.95703	2.24276	1.85202	2.33023	1.74068
2.0	2.21808	2.21808	2.30648	2.126	2.39162	2.02975	2.47384	1.9287

Table 3 Variations of ϕ with load parameter μ at various amplitudes for short (L/ζ = 25) asymmetrical composite beams with simply supported end condition [0 deg/90 deg]

		$\mu = 0.0$		$\mu = 0.2$		$\mu = 0.4$		$\mu = 0.6$	
A_m	B_m	ϕ_1	ϕ_2	ϕ_1	ϕ_2	ϕ_1	ϕ_2	ϕ_1	ϕ_2
0.0	0.0	2	2	2.09762	1.89737	2.19089	1.78885	2.28035	1.67332
0.2	−0.1821	1.88134	1.88134	1.9848	1.77185	2.08313	1.65513	2.17703	1.52952
0.4	−0.3348	1.77936	1.77936	1.88842	1.66317	1.99151	1.53822	2.08953	1.40219
0.8	−0.5841	1.63744	1.63744	1.75534	1.51037	1.8658	1.37158	1.97008	1.21705
1.2	−0.7977	1.5954	1.5954	1.71619	1.46468	1.82901	1.32109	1.93528	1.15987
2.0	−1.2457	1.82218	1.82218	1.92882	1.7089	2.02987	1.58756	2.12611	1.45614

Table 4 Variations of ϕ with load parameter μ at various amplitudes for short (L/ζ = 25) asymmetrical composite beams with fixed-end condition [0 deg/90 deg]

	$\mu = 0.0$		$\mu = 0.2$		$\mu = 0.4$		$\mu = 0.6$	
A_m	ϕ_1	ϕ_2	ϕ_1	ϕ_2	ϕ_1	ϕ_2	ϕ_1	ϕ_2
0	2	2	2.09762	1.89737	2.19089	1.78885	2.28035	1.67332
0.2	2.00699	2.00699	2.10429	1.90474	2.19728	1.79667	2.28649	1.68167
0.4	2.02783	2.02783	2.12417	1.92668	2.21633	1.81992	2.3048	1.70649
0.8	2.10913	2.10913	2.20191	2.01207	2.29094	1.91009	2.37664	1.80234
1.0	2.1681	2.1681	2.25847	2.07381	2.34535	1.97501	2.42913	1.87101
2.0	2.60819	2.60819	2.68378	2.53035	2.75729	2.45003	2.8289	2.367

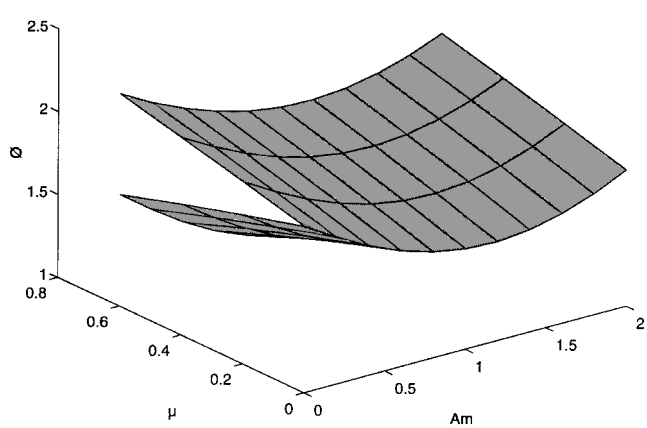

Fig. 2 Variation of ϕ with load parameters μ at various amplitudes for a short (L/ζ = 25) composite beam (cross ply 0 deg/90 deg) with SS ends.

and negative deflection cycles. Further, a softening type of nonlinearity for small amplitudes can be noticed, which changes to a hardening type at large amplitudes. Whereas these cross-ply beams with FF ends behaved like the ones studied earlier, the behavior of such beams with SS ends is quite different. For example, the region of stability increased initially with the increase in amplitude (up to $A_m = 1.2$) and then started decreasing. The increase in the stability region at $A_m = 1.2$ is nearly 22%, and at $A_m = 2.0$ it is only 10% compared with one at $A_m = 0.0$.

Concluding Remarks

A semi-analytical approach is proposed in this Note to investigate the nonlinear dynamic stability characteristics of asymmetrically laminated beams. The method has been successfully demonstrated and employed to compute the dynamic instability regions of various laminated beam configurations. In general, the instability region decreases with the increase in amplitude. Further, this reduction is more for beams with both of the ends SS; however, in the case of SS two-layer, cross-ply beams, this region initially increases with the increase in amplitude and then decreases. The proposed method

easily can be extended to investigate the dynamic stability behavior of plate and shells.

References

[1]Beliaev, N. M., "Stability of Prismatic Rods Subjected to Variable Longitudinal Forces," *Engineering Constructions and Structural Mechanics*, 1924, pp. 149–167.

[2]Bolotin, V. V., *Dynamic Stability of Elastic Systems*, Holden–Day, San Francisco, 1964, pp. 9–32.

[3]Beal, T. R., "Dynamic Stability of Flexible Missile Under Constant Pulsating Thrust," *AIAA Journal*, Vol. 3, No. 3, 1965, pp. 486–494.

[4]Peter, D. A., and Wu, J. J., "Asymptotic Solutions to a Stability Problem," *Journal of Sound and Vibration*, Vol. 59, No. 4, 1978, pp. 591–610.

[5]Reiss, E. L., and Matkowsky, B. J., "Nonlinear Dynamic Buckling of a Compressed Elastic Column," *Quarterly of Applied Mathematics*, Vol. 29, 1971, pp. 245–260.

[6]Rubenfield, L. A., "Nonlinear Dynamic Buckling of a Compressed Elastic Column," *Quarterly of Applied Mathematics*, Vol. 32, No. 2, 1974, pp. 163–171.

[7]Brown, J. E., Hutt, J. M., and Salama, A. E., "Finite Element Solution to Dynamic Stability of Bars," *AIAA Journal*, Vol. 6, No. 7, 1968, pp. 1423–1425.

[8]Sheinman, I., "Cylindrical Buckling Load of Laminated Columns," *Journal of Engineering Mechanics*, Vol. 115, No. 3, 1989, pp. 659–661.

[9]Singh, G., Rao, G. V., and Iyengar, N. G. R., "Large Amplitude Free Vibrations of Simply Supported Antisymmetric Cross Ply Plates," *AIAA Journal*, Vol. 29, No. 5, 1991, pp. 784–790.

[10]Bangera, K. M., and Chandrashekhara, K., "Nonlinear Vibration of Moderately Thick Laminated Beams Using Finite Element Method," *Finite Elements in Analysis and Design*, Vol. 9, 1991, pp. 321–333.

[11]Obst, A. W., and Kapania, R. K., "Nonlinear Static and Transient Finite Element Analysis of Laminated Beams," *Composite Engineering*, Vol. 2, 1992, pp. 375–389.

[12]Reddy, J. N., *Energy and Variational Methods in Applied Mechanics with an Introduction to FEM*, Wiley, New York, 1984, pp. 177–309.

S. Saigal
Associate Editor

Zeroth-Order Shear Deformation Theory for Plates

Rameshchandra P. Shimpi*
Indian Institute of Technology,
Powai, Mumbai 400 076, India

Introduction

PLATE analysis involving higher-order effects such as shear is an involved and tedious process. Even the considerably simple and well-known theories such as Reissner's[1] and Mindlin's[2] require solving two differential equations involving two unknown functions and involve the use of a shear coefficient for approximately satisfying the constitutive relationship between shear stress and shear strain. However, it is possible to take into account the higher-order effects and yet keep the complexity to a considerably lower level. Great simplification is possible if axial displacement is allowed to be influenced also by shear force and if proper use is made of the relationships (which always hold, regardless of the plate theory that is used) between moments, shear forces, and loading on the plate.

In the theory to be developed, the governing differential equation is of fourth order (as is the case in classical plate theory). In the governing equation only lateral deflection, plate physical properties, and lateral loading are going to figure. Therefore, the theory developed will be called the zeroth-order shear deformation theory (ZSDT) for plates.

The essential differences between Librescu's[3] approach and the present can be summarized as follows:

Librescu's approach makes use of weighted lateral displacement, whereas the ZSDT approach uses the lateral displacement itself, and therefore the approach is physically more meaningful.

In contrast to Librescu's approach, the ZSDT approach utilizes—right from the formulation stage—only physically meaningful entities, e.g., lateral deflection and shear forces.

Note that Reissner's formulation comes out as a special case of Librescu's formulation, whereas classical plate theory comes out as a special case of ZSDT formulation. Therefore, it is the opinion of the author that, in the context of a finite element solution of thin-plate problems, if finite elements based on Librescu's approach are used, the elements will be prone to shear locking, whereas the finite elements based on the ZSDT will be free from shear locking.

Plate Under Consideration

Consider a plate of length a, width b, and thickness h of homogeneous isotropic material. In the $o-x-y-z$ Cartesian coordinate system, the plate occupies a region

$$0 \le x \le a, \qquad 0 \le y \le b, \qquad -h/2 \le z \le h/2 \tag{1}$$

The plate is loaded on surface $z=-h/2$ by a lateral load of intensity $q(x, y)$ acting in the z direction. The plate can have any meaningful boundary conditions at edges $x=0, a$ and $y=0, b$. The modulus of elasticity E, shear modulus G, and Poisson's ratio μ are related by $G=E/[2(1+\mu)]$. The plate rigidity D is defined by $D=Eh^3/[12(1-\mu^2)]$.

Equilibrium Equations for the Plate

The moments M_x, M_y, and M_{xy} and shear forces Q_x and Q_y are defined as

$$\begin{Bmatrix} M_x \\ M_y \\ M_{xy} \\ Q_x \\ Q_y \end{Bmatrix} = \int_{z=-h/2}^{z=h/2} \begin{Bmatrix} \sigma_x z \\ \sigma_y z \\ \tau_{xy} z \\ \tau_{zx} \\ \tau_{yz} \end{Bmatrix} \mathrm{d}z \tag{2}$$

It is worthwhile to note certain relationships between moments, shear forces, and loading:

$$\frac{\partial M_x}{\partial x} + \frac{\partial M_{xy}}{\partial y} - Q_x = 0 \tag{3}$$

$$\frac{\partial M_{xy}}{\partial x} + \frac{\partial M_y}{\partial y} - Q_y = 0 \tag{4}$$

$$\frac{\partial Q_x}{\partial x} + \frac{\partial Q_y}{\partial y} + q = 0 \tag{5}$$

Equations (3–5) can be construed to be the gross equilibrium equations for any plate. As such, in the context of the classical plate theory, Eqs. (3–5) are well-known relations.[4] Note that the relations hold for any plate theory including any higher-order plate theory.

Assumptions for ZSDT for Plates

The following are the assumptions involved in respect to ZSDT:

1) The displacements are small, and therefore the strains involved are infinitesimals.

2) The lateral displacement w is a function of coordinates x and y only.

3) In general, stress σ_z is negligible in comparison with σ_x and σ_y. Therefore, for linearly elastic isotropic material it is possible to use the relations

$$\sigma_x = [E/(1-\mu^2)](\epsilon_x + \mu\epsilon_y)$$

$$\sigma_y = [E/(1-\mu^2)](\epsilon_y + \mu\epsilon_x)$$

4) The displacement u in the x direction and displacement v in the y direction each consists of two components.

Received Nov. 17, 1997; revision received Oct. 1, 1998; accepted for publication Dec. 27, 1998.

*Associate Professor, Aerospace Engineering Department.